Transient Photovoltage in Perovskite Solar Cells: Interaction of Trap-Mediated Recombination and Migration of Multiple Ionic Species

Daniel Walter*[1], Andreas Fell[2,3], Yiliang Wu[1], The Duong[1], Chog Barugkin[1], Nandi Wu[1], Thomas White[1], Klaus Weber[1]

[1]Research School of Engineering, Australian National University, Canberra, Australia

[2]Fraunhofer Institute for Solar Energy Systems, Freiburg, Germany

[3]AF simulations, Landstr. 12, 79232 March, Germany

*Corresponding author: daniel.walter@anu.edu.au

Supplementary Information

S1 Details on Quokka3 model and implemented drift diffusion equations

Electron-hole recombination occurs via intrinsic (e.g. Auger and radiative) processes, as well as through trapping centres modelled after Shockley-Read-Hall (SRH) statistics [1]. Radiative recombination is modelled by

$$R_{rad} = Bnp \qquad (1)$$

While Auger recombination is modelled by

$$R_{Aug} = C_n n(np - n_i^2) + C_p p(np - n_i^2) \qquad (2)$$

SRH can be modelled in its general or simplified form, the general form accounting for the effect of trapping on the charge density and resulting in unequal recombination rates for electrons and holes R_{el} and R_{hol}. In principle, the simplified form of SRH recombination is not applicable where trap densities are within one order-of-magnitude of the charge carrier density [2], which broadly applies to the simulations performed here. However, we found that the generalised form was not required to replicate the voltage transients. Because the simplified form of SRH recombination is less computationally difficult, we have used it throughout, following the expression

$$R_{SRH} = \frac{pn - n_{i,eff}^2}{\tau_n(p_1 + p) + \tau_p(n_1 + n)} \qquad (3)$$

where the electron and hole lifetimes are computed from $\tau_{n/p} = 1/(N_t \sigma_{n/p} v_t)$.

In the drift-diffusion model, a general system of 6 nonlinear differential equations comprises the continuity equations for the 4 charge carrier densities

$$q\frac{dn}{dt} = q(G - R_{el}) - \frac{dJ_{el}}{dz}, \tag{4}$$

$$q\frac{dp}{dt} = q(G - R_{hol}) + \frac{dJ_{hol}}{dz}, \tag{5}$$

$$q\frac{dc_{an}}{dt} = -\frac{dJ_{an}}{dz}, \tag{6}$$

$$q\frac{dc_{cat}}{dt} = \frac{dJ_{cat}}{dz}, \tag{7}$$

the continuity equation for the trapped electron density (if implemented with general SRH statistics)

$$\frac{dn_t}{dt} = R_{el} - R_{hol}, \tag{8}$$

and the Poisson equation for the electric potential

$$\frac{d}{dz}\left(-\varepsilon\frac{d\varphi_e}{dz}\right) = q(N_D - N_A + p - n + c_{cat} - c_{an} - n_t). \tag{9}$$

The current densities for all charge carriers due to drift and diffusion can be expressed via the quasi-Fermi potentials (i.e. the electrochemical potential) gradient, and the carrier concentration and mobility as

$$J_X = qc_X\mu_X\frac{d\phi_X}{dz}. \tag{10}$$

The carrier densities are calculated via Fermi-Dirac statistics for electrons and holes

$$n = N_c F_{1/2}\left(\frac{q\phi_{el}+E_c}{kT}\right), \tag{11}$$

$$p = N_v F_{1/2}\left(-\frac{q\phi_{hol}+E_v}{kT}\right), \tag{12}$$

and Boltzmann statistics for ions

$$c_{an} = N_{0,an}\exp\left(\frac{q(\phi_{an}+\varphi_e)}{kT}\right), \tag{13}$$

$$c_{cat} = N_{0,cat}\exp\left(-\frac{q(\phi_{an}+\varphi_e)}{kT}\right). \tag{14}$$

The generation rate G is a user-input into the model.

The electron and hole transport layers (ETL and HTL) are simplified to a metal-semiconductor (MS) boundary condition characterized by an effective barrier height and surface recombination properties. Majority carrier transport over the boundary is defined via thermionic emission

$$J_{maj} = A_0 T^2 \exp\left(-\frac{\Phi_B}{kT}\right)\left[\exp\left(\frac{\varphi_{cont}-\phi_{maj}}{kT/q}\right)-1\right] \pm J_{rec}, \quad (15)$$

and the band edge energies E_c and E_v as

$$E_{c/v} = q\varphi_{cont} \pm \Phi_B. \quad (16)$$

The barrier-height Φ_B can either be directly defined by the user, or derived from the work-function of the contact material. The latter is equivalent to the Fermi-level within the ETL / HTL, assuming negligible Fermi-level pinning:

$$\Phi_B = \pm\left(E_{c/v} - WF\right). \quad (17)$$

Independently of the contact physics, surface recombination is modelled via the simplified SRH mechanism. Only electrons and holes in the perovskite layer are available for recombination (i.e. there is no cross-recombination between hole and electron populations in the transport layers).

$$J_{rec} = \frac{pn - n_{i,eff}^2}{S_{n0}(p_1+p)+S_{p0}(n_1+n)}. \quad (18)$$

As mentioned above, conservation of the integral ion concentration within the perovskite layer is assumed, meaning that the boundary conditions for ion transport is defined by zero current flow

$$J_{cat} = J_{an} = 0. \quad (19)$$

A finite-differences scheme on a non-equidistant mesh is applied, and the resulting system of nonlinear equations is solved by a Newton linesearch algorithm using the C++ library PETSC. Numerical robustness is achieved by supplying an analytical Jacobian, successfully addressing the numerical challenge of a full discretization and direct numerical solution of the model even within the Debye layer, and thus not requiring asymptotic approximations (e.g. as in [3,4]).

To compute the J-V hysteresis, the cell was swept instantaneously (i.e. no ion movement was allowed) to short circuit. Once at short circuit (terminal voltage = 0V), the ion population was allowed to evolve for 300s, to replicate the stabilisation of the cell at short-circuit before the rapid forward sweep. The cell voltage was then swept back to open-circuit with no ion movement.

Finally, we note that an assumption of this model is that the built-in electric field is fully compensated in the perovskite absorber, and excludes capacitive effects in the transport layers. This is a consequence of assuming metal-semiconductor contacts. This may affect the computed ion distributions, as the energy levels at the transport-layer side of the interfaces are not influenced by the

ion accumulation. This approach has been used in previous works, e.g. [4,5], and we believe is a suitable first-order approximation of the interface physics. It does not affect the general conclusion of this work that the evolution of the net ion population following illumination is significantly influential on SRH recombination in the absorber.

Table S1: Summary of material parameters

Parameter	Symbol	Value	Reference
Perovskite absorber thickness		400 nm	
Electron affinity	E_{EA}	3.8 eV	
Conduction Band Density of States	N_c	2.2×10^{18} cm^{-3}	6
Valence Band Density of States	N_v	1.2×10^{19} cm^{-3}	6
Band gap	E_g	1.6 eV	7
Relative permittivity	ε_r	25	8
Electron mobility	$\mu_{electron}$	20 cm^2/Vs	9
Hole mobility	μ_{hole}	20 cm^2/Vs	9
Radiative recombination coefficient	B	6.8×10^{-10} cm^3 s^{-1}	10
Auger recombination coefficients	C_n, C_p	0.5×10^{-28} cm^{-6}	11
Work Function, Electron Transport Layer	$W_{F,ETL}$	3.9 eV	
Work Function, Hole Transport Layer	$W_{F,HTL}$	5.2 eV	
Generation	G	3×10^{21} cm^{-3} s^{-1}	
Trap energy level, relative to mid-gap	E_t-E_i	0 eV	
Capture cross-section, electrons, holes	$\sigma_{n,p}$	10^{-15} cm^2	
Net bulk doping	N_A-N_D	0	

S2 JV Hysteresis in the presence of dominant interface recombination

The current density-voltage (JV) hysteresis of figure 3b of the main manuscript may be indicative of high interface recombination. The focus in our discussion is on the influence of bulk SRH recombination on the transient voltage response. However, our model can replicate the substantial drop in open-circuit voltage, in addition to the absence of the S-shaped JV under short-circuit ion accumulation, in a device with high interface recombination (S_n=S_p=10^5 cm/s), and low electron-hole mobility ($\mu_{electron}$=μ_{hole}=1 cm^2/Vs). The high interface recombination, in the presence of mobile ions, manifests a substantial change in open-circuit voltage between the SC and OC-biased JV curves (by the same mechanism as discussed in section S3, below). The low electron-hole mobility is necessary to reduce charge carrier collection, which in turn flattens the shape of the J-V curve, as a larger quantity of photogenerated electronic charge is lost to recombination at all biases. The modified simulation parameters, relative to those tabulated in table S1, are presented in table S2.

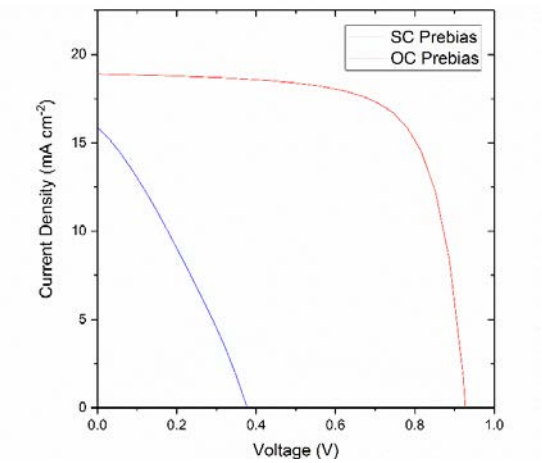

Figure S1: Simulated JV hysteresis for device with high interface recombination and low bulk mobility.

Table S2: Modified simulation parameters for figure S1

Parameter	Symbol	Value	Reference
Cation Concentration	C_{cat}	1×10^{20} cm^{-3}	
Anion Concentration	C_{an}	1×10^{20} cm^{-3}	
Hole Mobility	μ_{hole}	1 cm^2/Vs	
Electron Mobility	$\mu_{electron}$	1 cm^2/Vs	

S3 A monotonic slow rise of open-circuit voltage following illumination

The literature also describes a third characteristic OCVT, in which the open-circuit voltage initially rises rapidly to a moderate voltage (e.g. ~0.5V), then rises slowly to steady-state[12,13]. The total rise in the voltage is on the order of hundreds of millivolts, by comparison to a variation on the order of tens of millivolts measured in the Type A and B OCVTs. Our model replicates the characteristic and the order of magnitude of this voltage rise in a device in which interface recombination is dominant over bulk recombination. To illustrate this, we simulated a perovskite absorber in which the trap defect density of the bulk is reduced to zero, and the interface recombination increased, with $S_n=S_p=10^5$ cm/s. Figure S2 plots the transient open-circuit voltage response of this device under a range of illumination levels from 0.02 to 1 suns-equivalent, to approximate the experimental conditions of the data presented in figure 1a of *Pockett et al*[12]. We see that the same general trend is observed: changing illumination shifts both the initial voltage that the device approaches within microseconds of illumination, as well as the voltage of the device after 200s of illumination. To approximate the time scale of the trend of reference 12, the ion parameters and interface work functions were adjusted, as tabulated in table S3.

The simulations demonstrate that ion movement affects the strength of interface recombination. An initial discussion of this effect was provided in a previous work[14], while a more detailed explanation of the mechanisms revealed by our modelling in the context of transient photocurrent measurements will be provided in a forthcoming work[15].

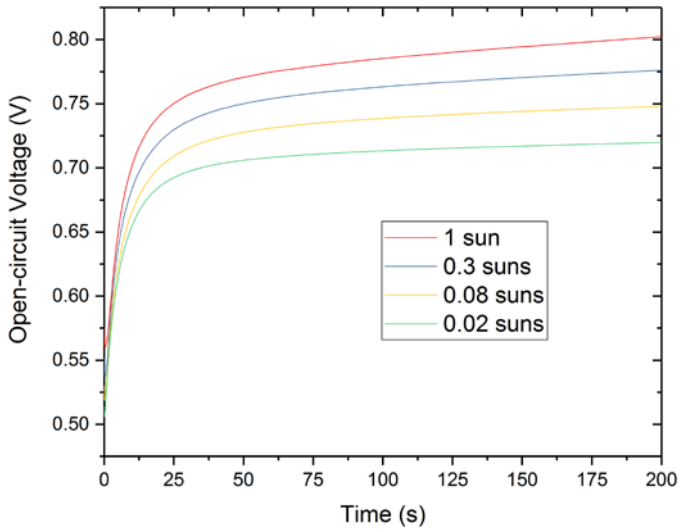

Figure S2: Slow voltage rise for a device in which surface recombination is dominant, illustrating the dependence of illumination on the OCVT.

Table S3: Modified simulation parameters for figure S2

Parameter	Symbol	Value	Reference
Cation Concentration	C_{cat}	1.2×10^{20} cm^{-3}	
Anion Concentration	C_{an}	1.2×10^{20} cm^{-3}	
Cation Mobility	μ_{cat}	6×10^{-10} cm^{-3}	
Anion Mobility	μ_{an}	1×10^{-15} cm^{-3}	
Work Function, Electron Transport Layer	$W_{F,ETL}$	3.8 eV	
Work Function, Hole Transport Layer	$W_{F,HTL}$	5.4 eV	

References

(1) Shockley, W.; Read, W. T. Statistics of the Recombinations of Holes and Electrons. *Phys. Rev.* **1952**, *87*, 835–842.

(2) Macdonald, D.; Cuevas, A. Validity of Simplified Shockley-Read-Hall Statistics for Modeling Carrier Lifetimes in Crystalline Silicon. *Phys. Rev. B* **2003**, *67*, 075203.

(3) J. O'Kane, S. E.; Richardson, G.; Pockett, A.; G. Niemann, R.; M. Cave, J.; Sakai, N.; E. Eperon, G.; J. Snaith, H.; M. Foster, J.; J. Cameron, P.; et al. Measurement and Modelling of Dark Current Decay Transients in Perovskite Solar Cells. *J. Mater. Chem. C* **2017**, *5*, 452–462.

(4) Richardson, G.; O'Kane, S. E. J.; Niemann, R. G.; Peltola, T. A.; Foster, J. M.; Cameron, P. J.; Walker, A. B. Can Slow-Moving Ions Explain Hysteresis in the Current–voltage Curves of Perovskite Solar Cells? *Energy Environ. Sci.* **2016**, *9*, 1476–1485.

(5) Neukom, M. T.; Züfle, S.; Knapp, E.; Makha, M.; Hany, R.; Ruhstaller, B. Why Perovskite Solar Cells with High Efficiency Show Small IV-Curve Hysteresis. *Sol. Energy Mater. Sol. Cells* **2017**, *169*, 159–166.

(6) Zhou, Q.; Jiao, D.; Fu, K.; Wu, X.; Chen, Y.; Lu, J.; Yang, S. Two-Dimensional Device Modeling of CH3NH3PbI3 Based Planar Heterojunction Perovskite Solar Cells. *Sol. Energy* **2016**, *123*, 51–56.

(7) Lee, M. M.; Teuscher, J.; Miyasaka, T.; Murakami, T. N.; Snaith, H. J. Efficient Hybrid Solar Cells Based on Meso-Superstructured Organometal Halide Perovskites. *Science* **2012**, *338*, 643–647.

(8) Onoda-Yamamuro, N.; Matsuo, T.; Suga, H. Dielectric Study of CH3NH3PbX3 (X = Cl, Br, I). *J. Phys. Chem. Solids* **1992**, *53*, 935–939.

(9) Staub, F.; Hempel, H.; Hebig, J.-C.; Mock, J.; Paetzold, U. W.; Rau, U.; Unold, T.; Kirchartz, T. Beyond Bulk Lifetimes: Insights into Lead Halide Perovskite Films from Time-Resolved Photoluminescence. *Phys. Rev. Appl.* **2016**, *6*, 044017.

(10) Crothers, T. W.; Milot, R. L.; Patel, J. B.; Parrott, E. S.; Schlipf, J.; Müller-Buschbaum, P.; Johnston, M. B.; Herz, L. M. Photon Reabsorption Masks Intrinsic Bimolecular Charge-Carrier Recombination in CH3NH3PbI3 Perovskite. *Nano Lett.* **2017**, *17*, 5782–5789.

(11) Johnston, M. B.; Herz, L. M. Hybrid Perovskites for Photovoltaics: Charge-Carrier Recombination, Diffusion, and Radiative Efficiencies. *Acc. Chem. Res.* **2016**, *49*, 146–154.

(12) Pockett, A.; E. Eperon, G.; Sakai, N.; J. Snaith, H.; M. Peter, L.; J. Cameron, P. Microseconds, Milliseconds and Seconds: Deconvoluting the Dynamic Behaviour of Planar Perovskite Solar Cells. *Phys. Chem. Chem. Phys.* **2017**, *19*, 5959–5970.

(13) Stranks, S. D.; Burlakov, V. M.; Leijtens, T.; Ball, J. M.; Goriely, A.; Snaith, H. J. Recombination Kinetics in Organic-Inorganic Perovskites: Excitons, Free Charge, and Subgap States. *Phys. Rev. Appl.* **2014**, *2*, 034007.

(14) Wu, Y.; Shen, H.; Walter, D.; Jacobs, D.; Duong, T.; Peng, J.; Jiang, L.; Cheng, Y.-B.; Weber, K. On the Origin of Hysteresis in Perovskite Solar Cells. *Adv. Funct. Mater.* **2016**, *26*, 6807–6813.

(15) De Bastiani, Michele; Aydin, Erkan; Allen, Thomas; Walter, Daniel; Fell, Andreas; Peng, Jun; Gasparini, Nicola; Troughton, Joel; Baran, Derya; Weber, Klaus; et al. Ions, Charge Accumulation, and Transient Currents: The Role of Contact Passivation in Perovskite Solar Cells. *Submitted* **2018**.